Modelling of free surface proximity and wave induced velocities around a horizontal axis tidal stream turbine

J. Whelan[1], M. Thomson [2] J. M. R. Graham[1] and J. Peiró[1]

[1] Department of Aeronautics
Imperial College London
E-mail: j.whelan,m.graham,j.peiro@imperial.ac.uk

[2]Garrad Hassan Ltd.
E-mail: mat.thomson@garradhassan.com

Abstract

The aim of this work is to model the flow field around a horizontal axis tidal stream turbine to include the effects of both free surface proximity and wave induced velocities. Theoretical results are presented for the case of a linear array of tidal stream turbines that account for the proximity of the free surface and the seabed. The theory is then developed further to account for wave induced velocities and the resultant unsteady loading on a turbine. The theoretical results are compared to open channel flow experimental results. The flow field has been first experimentally simulated using various resistance discs. These results will be complemented by more detailed measurements using a model turbine. A combination of oscillatory flow and current is used to simulate the effects of wave and current motion on the turbine. The work on free surface proximity culminates in a blockage correction for free surface flows. The extension of this theory for inclusion of wave induced velocities provides a characterisation of the unsteady loading on the turbine due to the wave motion. Incorporation of the corrections for free surface proximity into a blade element code is discussed.

Nomenclature

D	=	diameter
b	=	transverse spacing
z_t	=	hub depth
z_1	=	depth upstream of the turbine
z_2	=	depth downstream of the turbine
δz	=	$z_1 - z_2$
s_1	=	width of streamtube upstream
s_w	=	width of streamtube downstream
s_t	=	equivalent 2-D turbine diameter (see B)
U_1	=	U = upstream velocity
U_t	=	βU = velocity at turbine
U_w	=	αU = wake velocity
U_2	=	τU = velocity outside of wake
k	=	resistance of the porous gauze
$\dot{m}$	=	flow rate
C_T	=	coefficient of thrust
C_P	=	coefficient of power
C_M	=	coefficient of added mass
B	=	$\frac{s_t}{z_1}$ = blockage ratio
F_1	=	$\frac{U_1^2}{g z_1}$ = upstream Froude number
Re	=	Reynolds number (based on disc diameter, D)
a	=	axial induction factor
ω	=	frequency of incident waves
k_o	=	wave number of incident waves
$\hat{z}_1$	=	amplitude of incident waves
H	=	$2\hat{z}_1$ = wave height
ϕ	=	potential
Δ	=	$(\,)_- - (\,)_+$
i	=	$\sqrt{-1}$

© Proceedings of the 7th European Wave and Tidal Energy Conference, Porto, Portugal, 2007

Introduction

In 2005 a study commissioned by the Carbon Trust estimates the total extractable UK tidal stream resource at approximately 22 TWh per year, which represents 6% of the UK electricity demand [1]. Tidal-stream flows are extremely predictable thus making them attractive for optimised energy conversion via horizontal-axis rotors [2]. Such devices will often operate in relatively shallow water where tidal currents are strongest and therefore be in the vicinity of a free-surface and subject to passing waves. The actuator disc distributes the loading of the turbine blades uniformly over a disc which acts as a discontinuity in pressure in the flow. It has been employed in various similar engineering applications [3], such as the modelling of wind turbines and ship propellers and it is again applicable here. A porous plate is frequently used as an analogue for an actuator disc and hence turbine rotor. It is particularly useful where small model scales would lead to unrepresentatively low blade Reynolds numbers in the latter case.

1 Modelling free-surface proximity

1.1 Theoretical model

We consider an array of horizontal axis rotors of diameter D, transverse spacing b, to be situated across a tidal stream at hub depth z_t (measured from the upstream mean free surface) in water of depth z_1, as shown in Figure 1. These rotors will be represented by actuator discs. Where the rotor spacing is fairly close a first approximation for the effects of free-surface and sea bed proximity can be obtained by considering a two-dimensional (transversely averaged) flow, as shown in Figure 2, where the area of the 'actuator (or resistance) strip' per unit transverse width of the flow is equal to the area occupied by rotor discs per unit width (i.e. the same blockage ratio):

$$B = \frac{\frac{\pi D^2}{4}}{z_1 b} = \frac{s_t}{z_1} \tag{1}$$

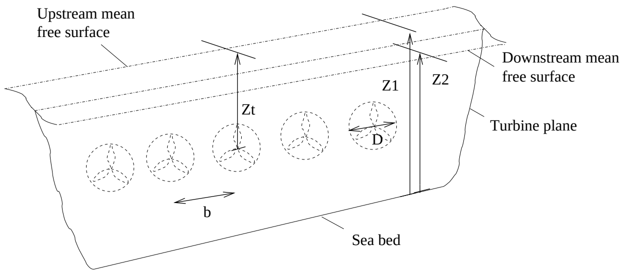

Figure 1: Diagram of array of rotors within a channel.

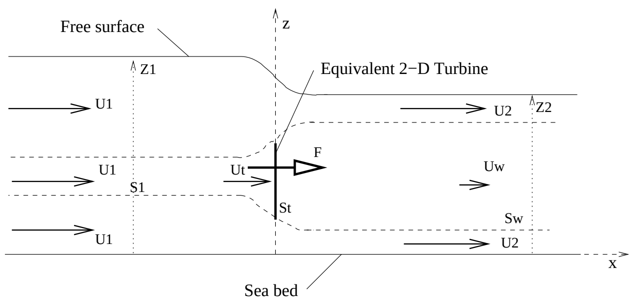

Figure 2: Schematic of 2D flow approximation.

By consideration of continuity, Bernoulli and momentum, a quartic equation in terms of τ can be derived, which once solved predicts the height drop due to the turbine's presence as well as the device characteristics such as C_t and hence C_p.

The pressure drop across a porous gauze is determined by means of a resistance coefficient, k, analogous to a drag coefficient

$$\Delta p = \frac{1}{2} k U_t^2 \tag{2}$$

1.1.1 Derivation

Applying continuity to the outside streamtube gives

$$U(z_1 - s_1) = \tau U(z_2 - s_w) \tag{3}$$

and then applying continuity to the inside streamtube gives

$$Us_1 = \beta U s_t = \alpha U s_w \tag{4}$$

rearranging (3) and (4) gives

$$\beta = \frac{[z_1(\tau - 1) - \tau \delta z]\alpha}{(\tau - \alpha)s_t} \tag{5}$$

Applying Bernoulli along the free surface gives height drop between z_1 and z_2

$$\delta z = \frac{U^2}{2g}(\tau^2 - 1) \tag{6}$$

and then applying Bernoulli along the central streamline gives the force on the turbine

$$F = s_t(gh + \frac{1}{2}U^2(1 - \alpha^2)) \tag{7}$$

The force on the turbine can also be obtained by applying conservation of momentum to a control volume surrounding the turbine and passing through the free surface

$$F = \sum pA - \sum \dot{m}V \tag{8}$$

Equation (8) can be written as

$$\begin{aligned} F &= \int_0^{z_1} (p_a + gz)dz - \int_0^{z_2} (p_a + gz)dz \\ &\quad - p_a(z_1 - z_2) - \dot{m}_{out}V_{out} + \dot{m}_{in}V_{in} \\ &= \frac{1}{2}gz_1^2 - \frac{1}{2}gz_2^2 - (z_2 - s_w)(\tau U)^2 \\ &\quad - s_w(\alpha U)^2 + z_1 U^2 \\ &= \frac{1}{2}g(2z_1\delta z - (\delta z)^2) + U^2 z_1(1 - \tau) \\ &\quad + \beta U^2 s_t(\tau - \alpha) \end{aligned}$$

Equating (7) and (8) and substituting for β by equation (5) and δz by equation (6) leads to a quartic in τ of the form

$$c_4\tau^4 + c_3\tau^3 + c_2\tau^2 + c_1\tau + c_0 = 0,$$

where

$$\begin{aligned} c_4 &= \frac{F_1}{8} \\ c_3 &= \frac{\alpha F_1}{2} \\ c_2 &= \frac{B}{2} - \frac{1}{2} - \frac{F_1}{4} \\ c_1 &= 1 - \alpha - \frac{\alpha F_1}{2} \\ c_0 &= \alpha - \frac{1}{2} + \frac{F_1}{8} - \frac{\alpha^2 B}{2} \end{aligned}$$

1.2 Verification of theory

1.2.1 Comparison with limit cases

As the height is increased, whilst maintaining a constant cross-sectional area of the turbine (i.e. the case of decreasing the blockage ratio to zero) the results from the free-surface proximity model approximate the well-known case of an actuator disc in unbounded flow (i.e. the Betz limit, where $C_P = \frac{16}{27}$ [4]) as shown in Figure 3. The higher blockage ratio lines in figure 3 also have maxima. For example a blockage ratio of 0.25 has a maximum C_P of 1.08 at a resistance coefficient of 7.4.

The free-surface proximity model has also been verified for the case of a blockage ratio of 1, against a 2-D analysis which considers the case of a gauze placed across the entirity of the channel. The two different analyses agree up to a resistance coefficient, $k = 4$, which corresponds to the “brake-state” for a turbine.

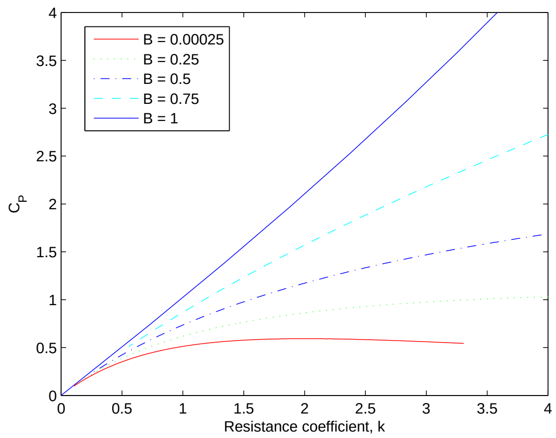

Figure 3: C_P as a function of k, for varying blockage ratios, at F_1 = 0.0229.

1.2.2 Comparison with experiments

Experiments were carried out in the water flume in Imperial College, which has a working section 0.6m wide, 0.64m deep and 9m long. The flume was run at flow speeds up to 0.72m/s, corresponding to a Froude number of 0.083 at full depth. Measurements of axial force were made on discs of varying resistance coefficient, k, with a diameter of 0.4m.

Determination of the resistance coefficient, k

There are various methods for determining the resistance coefficient, e.g

1. Via published correlations relating k to the open area ratio, θ, and published measured data for gauzes and porous plates [5]. The most well-known correlation is given below as equation (10).
2. Via wind tunnel measurements - e.g. placing a sheet of the porous material across a duct, and measuring the pressure upstream and downstream.
3. Via water flume measurements - e.g. placing a sheet of the porous material across the entire channel (i.e. B = 1) and taking measurements of axial force and flow speed.

The theoretical relationship between resistance coefficient and drag coefficient (which in this case is analogous to C_T) is [5]

$$C_t = \frac{k}{(1 + \frac{1}{4}k)^2} \tag{9}$$

Taylor’s publications on porosity do not provide a definitive relationship between open area ratio, θ, and resistance coefficient, k, however a first approximation often cited is [5]

$$\theta^2 = \frac{1}{1 + k} \tag{10}$$

The optimum efficiency state of a turbine operating in open-flow (the Betz limit) is related to k via equation (9) and found to be 2. A corresponding open-area ratio, θ = 0.58 is then predicted using equation (10). In the first instance, perforated plate material with this open-area ratio was chosen for the turbine simulation. The resistance coefficient was then confirmed experimentally via water flume measurements (at Re = 2 x 10^5). The resistance factor, k, was found to be 1.8. This value is used in the analysis that follows.

In addition to the perforated plate, two other materials were used to construct the 0.4m circular discs (wire grid and expanded metal). Wind tunnel measurements were performed on these two materials (at Re = 5 x 10^5). Figure 4 shows the experimentally determined k factors for the various porous discs used in the experiments. The straight line (equation (10)) is a frequently used correlation (i.e. there is no firm theoretical basis), however the tests agree well for the perforated plate and wire grid samples. The experimentally determined k for the expanded metal sample deviates from Taylor’s first approximation, however the sample consisted of diamond shaped holes which may account for this.

Experimental results

The disc form provides a representation of the turbine. In order to provide a test of the accuracy of using a 2-D theoretical model to represent flow about an array of discs, measurements of axial force were also made on a 2-D strip of the same porous material and equal blockage to the disc in the flume, deployed across the whole width of the flume. The force measurements from both the disc and the strip correspond to one another closely as expected for higher Froude numbers and shown in figure 5 . These measurements confirm the 2-D analogy and are also close to those predicted by the free-surface proximity model.

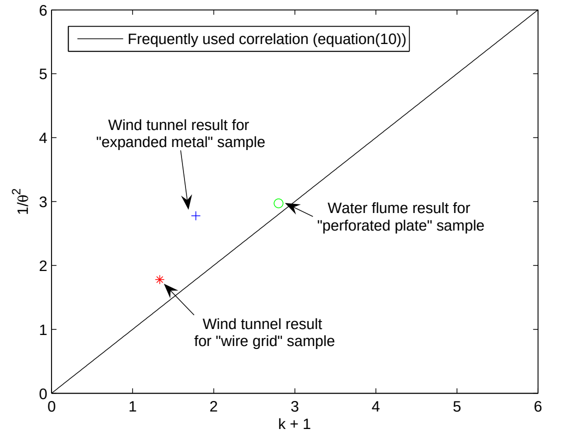

Figure 4: θ vs k, experimental points and Taylor's predicted relationship.

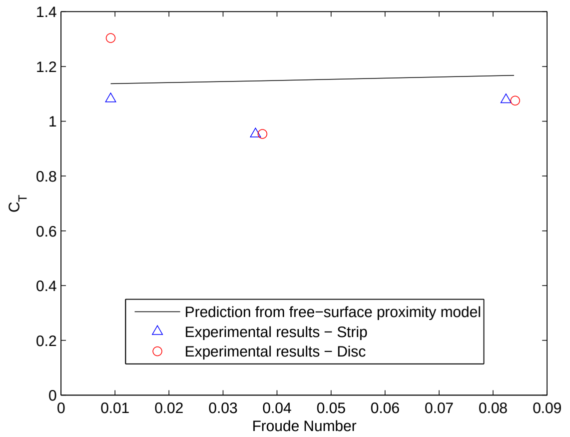

Figure 5: C_T vs Fr for varying blockage ratios.

1.3 Blockage correction to B.E.M

Figure 6 is an initial attempt to use the two-dimensional free-surface proximity model to provide a correction factor for blockage to serve as an input to Blade Element Momentum industrial codes commonly used for design purposes.

The more commonly known axial induction factor, a, is related to β by:

$$a = 1 - \beta \tag{11}$$

As expected, Figure 6 demonstrates that the turbine will experience an increased C_T for the same axial induction factor, a, as blockage ratio increases. A realistic blockage ratio for tidal turbine operation in arrays is 0.125. At an induction factor of $\frac{1}{3}$ (corresponding to the Betz limit) a turbine is likely to experience an increased C_t by 28%.

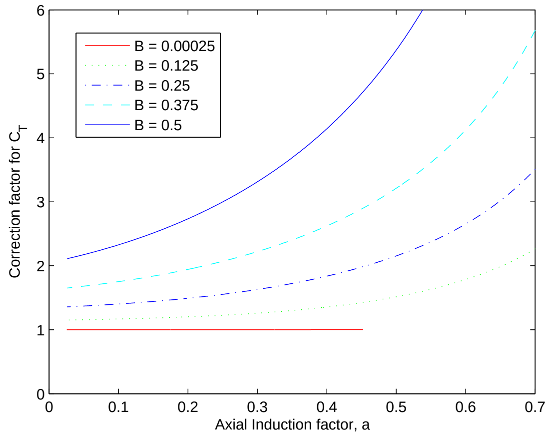

Figure 6: Correction factor vs axial induction factor for varying blockage ratios.

2 Interaction of free surface waves with a rotor array

As a stage towards evaluating the influence including diffraction of general incident free surface waves in addition to a mean current on an array of tidal stream turbines, the following analysis is presented for the interaction of a regular wave train incident normally on a horizontal 'actuator (resistance) strip' in the absence of the current. The resistance strip is the porous plate analogue of an array of horizontal axis rotors shown in Figure 2 and follows the same philosophy as applied to the steady flow cases in Section 1. In the case which is considered here it is assumed that there is no mean flow, the mean free surface is taken to be the plane $z = 0$ and the middle of the device is at a depth $z = -z_t$ from the upstream mean free surface. A regular wave train

$$z_1 = \hat{z}_1 e^{i(\omega t - k_o x)}$$

propagating in the positive x direction is incident on the device. The flow is assumed to be at high Reynolds number and is treated as inviscid.

The analysis follows the work of Chwang [6] for porous barriers. Linear wave theory is assumed and the velocity potential is defined

$$\phi = \hat{\phi}(x, z)e^{i\omega t}$$

Deep water will be assumed for simplicity, so therefore the dispersion relation is

$$k_o = \frac{\omega^2}{g}$$

and the potential for the incident waves is

$$\phi_1 = \hat{\phi}_1 e^{i(\omega t - k_o x)} e^{k_o z}$$

with

$$\hat{\phi}_1 = \frac{i\omega}{k_o}\hat{z}_1$$

A linear relationship is assumed to hold (Chwang [6]) between the pressure difference across the plate $-\rho\Delta\frac{\partial\phi}{\partial t}$ and the velocity $\frac{\partial\phi}{\partial x}$ through the plate $\Delta = (\ )_- - (\ )_+$ where $+$ and $-$ are the $x < 0$ and $x > 0$ faces of the plate. Thus

$$-\rho\Delta\frac{\partial\phi}{\partial t} = i\omega G\left(\frac{\partial\phi}{\partial x}\right)_{x=0;|z+z_t|\le\frac{s_t}{2}} \qquad (12)$$

where the complex constant of proportionality, G, represents the contributions from both the velocity-proportional loading and the inertia (added mass). Here $z = -z_t$ is the middle of the strip. G may be related to the viscous flows through the pores of the plate (Taylor [5]) or to a linearised representation of Morison's equation which is more appropriate for the low resistance coefficients representative of an actuator disc.

The potential is composed of five components

1. Incident waves

$$x \le 0;\ \ \phi_1 = \hat{\phi}_1 e^{i(\omega t - k_o x)} e^{k_o z} \qquad (13)$$

2. Reflected waves

$$x \le 0;\ \ \phi_R = \hat{\phi}_R e^{i(\omega t + k_o x)} e^{k_o z} \qquad (14)$$

3. Transmitted waves

$$x \ge 0;\ \ \phi_T = \hat{\phi}_T e^{i(\omega t - k_o x)} e^{k_o z} \qquad (15)$$

4. Eigensolution 1

$$x \le 0;\ \ \phi_- = \int_0^\infty A(\mu)(cos\mu z + \frac{k_o}{\mu} sin\mu z)e^{\mu x} d\mu \qquad (16)$$

5. Eigensolution 2

$$x \ge 0;\ \ \phi_+ = \int_0^\infty B(\mu)(cos\mu z + \frac{k_o}{\mu} sin\mu z)e^{-\mu x} d\mu \qquad (17)$$

Equations (16) and (17) are eigensolutions satifying the free surface boundary conditions and representing local disturbances around the plate which decay with distance and do not propagate away.

The two boundary conditions in the plane $x = 0$ of the plate are:

Pressure jump condition

$$\Delta\phi = \begin{cases} -G\frac{\partial\phi}{\partial x} & |\ z + z_t\ | \le \frac{s_t}{2} \\ 0 & |\ z + z_t\ | > \frac{s_t}{2} \end{cases} \qquad (18)$$

Continuity of velocity

$$\Delta\frac{\partial\phi}{\partial x} = 0 \qquad (19)$$

Substituting the potentials above (equations (13) - (17)) into (18) and (19) and non-dimensionalising

$$Z = \frac{2(z + z_t)}{s_t};\quad Z_o = \frac{-2z_t}{s_t};$$

$$\tilde{G} = \frac{G}{s_t};\quad \tilde{\mu} = \frac{s_t\mu}{2};\quad K_o = \frac{k_o s_t}{2};$$

$$C(\tilde{\mu}) = (1 + \tilde{\mu}\tilde{G})(cos\tilde{\mu}z_o + \frac{k_o}{\tilde{\mu}} sin\tilde{\mu}z_o)B(\mu)$$

results in a pair of integral equations for the unknown function $C(\tilde{\mu})$:

- for $|\ Z\ | \le 1$

$$C_o coshK_0 Z + \int_0^\infty C(\tilde{\mu})cos\tilde{\mu}Zd\tilde{\mu} = iK_o\tilde{G}\hat{\phi}_1 coshK_0 Z \qquad (20)$$

- for $|\ Z\ | > 1$

$$\frac{C_o coshK_0 Z}{1 + iK_o\tilde{G}} + \int_0^\infty \frac{C(\tilde{\mu})cos\tilde{\mu}Z}{1 + \tilde{\mu}\tilde{G}} d\tilde{\mu} = 0 \qquad (21)$$

where the disturbance has been assumed to be symmetric about $x = 0$ upstream and downstream and the symmetric (with respect to z) part of the solution about the mid-line of the plate has been selected to calculate the loading on the plate. The coefficient $C_o = (1 + iK_o\tilde{G})(\hat{\phi}_T - \hat{\phi}_1)$ is proportional to the part of the disturbance which propagates as a wave.

A solution of equations (20) and (21) can be obtained by using a series expansion of $C(\tilde{\mu})$ in terms of the Bessel functions $J_{(2n+1)}(\tilde{\mu})$ [7].

This procedure has been carried out here taking only the first term of the series to give an approximate solution for

$$\frac{\hat{\phi}_T}{\hat{\phi}_1} = 1 - \frac{iK_o\tilde{G}}{2 - 4coshK_o + \frac{(1+iK_o\tilde{G})}{(i+\tilde{G})} + \frac{1}{4K_o}}$$

The loading coefficient $\tilde{G}$ must be determined by experiments or by heuristic analysis.

2.1 Example evaluation

Morison's equation for the force F_X in the flow direction on a device (area A, volume V) in unsteady flow $U(t)$

$$F_X = \frac{1}{2}\rho U|U|AC_D + \rho\frac{dU}{dt}VC_M$$

can be converted to a similar equation for pressure difference Δp across the resistance strip in unsteady flow

$$\Delta p = \frac{k}{2}\rho\frac{\partial\phi}{\partial x}\left|\frac{\partial\phi}{\partial x}\right| + \rho C_M s_t\left(\frac{\partial^2\phi}{\partial t\,\partial x}\right)_{x=0} \qquad (22)$$

which extends the steady flow relationship (equation (2)) to unsteady flow. k is the resistance coefficient, C_M is an inertia coefficient including the added mass effect and the modulus sign is required for reversing flows.

Equation (22) may be linearised by replacing $|\frac{\partial \phi}{\partial x}|$ by some characteristic constant velocity here chosen to be $k_o \hat{\phi} e^{k_o z_t}$, thus

$$\Delta p = \frac{k_o}{2} k \rho \frac{\partial \phi}{\partial x} \hat{\phi} e^{k_o z_t} + \rho C_M s_t \frac{\partial^2 \phi}{\partial t \, \partial x}$$

The added mass coefficient C_M has not as yet been evaluated. For the present purposes C_M is assumed to be of similar size to the velocity dependent part of the loading.

The following example values have been used

k	=	2 (for max. C_P in unconstrained steady flow)
s_t	=	10 m
H	=	5 m
z_t	=	-7.5 m (as close to the surface as possible)
k_o	=	$\frac{2\pi}{60}$ m^{-1}

to give

$$\lambda \simeq 0.85 - 0.017i$$

The power coefficient representing the ratio of the mean power extracted by the device from the incident waves divided by the mean power in the incident waves is then calculated for this particular example to be

$$\begin{aligned} C_P &\simeq \Re(\lambda(1-\lambda)), where\ \lambda = \frac{\hat{\phi}_T}{\hat{\phi}_1} \\ &\simeq 0.128 \end{aligned}$$

3 Conclusions

Two dimensional 'actuator strip' theory has been presented for flow past an array of tidal stream turbines in close proximity to the free surface. The blockage effect due to the free surface and sea bed has been computed for steady flow, providing a correction to the wake induction factor used in Blade Element Momentul codes that are useful for industrial design purposes. As expected significant increases in power coefficient can result from the blockage effect. For surface wave induced flows an initial linearised analysis has been presented for the interaction of a regular wave train with the rotor array. This analysis can be used to provide an estimate of the oscillatory loading induced by the waves on the device and the amplitudes of the reflected and transmitted waves and will be developed further to combine with the steady current analysis.

References

[1] Carbon Trust. *UK Tidal Stream Resource Assessment*. Produced by Black and Veatch Ltd, 2005.

[2] Carbon Trust. *Variability of UK Marine Resources*. Produced by Environmental Change Institute, Oxford, 2005.

[3] R.E. Wilson and A.J. Lissaman. *Applied Aerodynamics of Wind Power Machines*. Oregon State University, 1974.

[4] T. Burton et al. *Wind energy handbook*. John Wiley and Sons, 2001.

[5] Edited by G.K.Batchelor. *The scientific papers of Sir Geoffrey Ingram Taylor*. Cambridge University Press, 1963.

[6] A.T. Chwang. A porous wave maker theory. *Journal of Fluid Mechanics*, 132(1):395–406, 1983.

[7] J.M.R. Graham. A lifting-surface theory for the rectangular wing in non-stationary flow. *The aeronautical quarterly*, XXII(1):83–100, 1971.